DEUTSCHES ELEKTRONEN-SYNCHROTRON DESY

DESY 74/18
May 1974

Quasi-Elastic Electron Scattering (e,e'p) and (e,e'd) from ^{6}Li in a Coincidence Experiment

by

F. H. Heimlich and E. Rössle
Fakultät für Physik der Universität Freiburg/Breisgau

M. Köbberling, J. Moritz, K. H. Schmidt, D. Wegener, D. Zeller
Institut für experimentelle Kernphysik der Universität (TH) und des Kernforschungszentrums Karlsruhe

J. K. Bienlein, J. Bleckwenn, H. Dinter
Deutsches Elektronen-Synchrotron DESY, Hamburg

2 HAMBURG 52 · NOTKESTIEG 1

To be sure that your preprints are promptly included in the
HIGH ENERGY PHYSICS INDEX ,
send them to the following address (if possible by air mail) :

DESY
Bibliothek
2 Hamburg 52
Notkestieg 1
Germany

Quasi-Elastic Electron Scattering (e,e'p) and (e,e'd) from ^{6}Li in a Coincidence Experiment

by

F.H. Heimlich and E. Rössle

Fakultät für Physik der Universität Freiburg/Breisgau

M. Köbberling, J. Moritz, K.H. Schmidt, D. Wegener*, D. Zeller

Institut für experimentelle Kernphysik der Universität (TH)

und des Kernforschungszentrums Karlsruhe

J.K. Bienlein, J. Bleckwenn, H. Dinter

Deutsches Elektronen-Synchrotron DESY, Hamburg

* Present address: CERN, Geneva (Switzerland)

Abstract

Coincidence cross sections for the reactions $^{6}Li(e,e'p)$ and $^{6}Li(e,e'd)$ have been measured in the region of quasi-elastic scattering. Using incident electrons of 2.5 and 2.7 GeV, the four-momentum transfers to the proton were 6.6 fm^{-2}, 10.0 fm^{-2} and 11.6 fm^{-2}. The proton coincidence data agree with shell model distributions assuming a Woods-Saxon potential and including short range nucleon-nucleon correlations. The best fit to the deuteron coincidence data is obtained with a cluster wave function for the p-nucleons and a harmonic oscillator wave function for the s-nucleons taking into account the deuteron yield from the s-shell. The ratio of the deuteron cross section from ^{6}Li divided by the elastic e-d-scattering cross section depends only slightly on the four-momentum transfer and has a value of ~ 2.

1. Introduction

The advantages of using electrons instead of strongly interacting particles as probes in nuclear structure studies are

- a well known basic interaction
- a small distortion of nuclear structure by the incoming and outgoing electron. In quasielastic processes only a heavy recoil particle suffers noticeable final state interaction.

Investigating the special problem of short-range correlations (SRC) of nucleons inside a nucleus, we can expect the following effects in connection with quasi-elastic electron scattering processes:

a) The nucleon momentum distribution given by the nuclear shell model is modified in its high-momentum part $\geq$ 200 MeV/c, since for nucleon-nucleon distances $\leq$ 1 fm short-range correlations introduce an interaction not included in the usual shell model description[1].

b) Two-particle emission is possible in a process caused by one-particle interaction - for instance by electron scattering assuming the one-photon exchange approximation. The emission of two nucleons after absorption of a virtual photon is improbable in the frame of the simple shell model, since the nucleons are assumed to move independently.

In looking for these effects the size of the probe should be comparable with that of the object to be analysed and the interaction time should be short enough to exclude nuclear rearrangement effects. These requirements are fulfilled by electrons in the GeV-range. We chose the (e,e'p)-reaction channel (quasi-elastic scattering with outgoing protons) for the determination of the momentum distri-

bution of the protons inside a ^{6}Li nucleus. In the simultaneously measured (e,e'd)-reaction channel, we restricted our measurements to the same quasi-elastic scattering kinematics as used in the (e,e'p)-case, i. e., we considered coincidence events kinematically corresponding to free e-d-scattering. The resulting deuteron production rate and the momentum distribution of p-n pairs in ^{6}Li should yield information about nucleon-nucleon interactions by comparison with models. A measurement of single-particle binding energies was not planned because of the finite energy resolution due to the primary beam and the electron spectrometer. ^{6}Li has been chosen as target nucleus for the following reasons:

- the final state interactions should be relatively small,
- the narrow nucleon-momentum distribution allows the separation of deuterons from protons in our experimental arrangement,
- the existence of a (α+d)-cluster structure is well known.

The previous quasi-elastic (e,e'p)-measurements were primarily concerned with single particle binding energies[2-4,46]. After the preliminary publication of the data of this experiment[47], other angular and momentum distributions obtained from ^{6}Li(e,e'p) at 1.2 GeV [5] and 0.7 GeV [6] were also published. In addition, momentum distributions have been obtained from quasi-elastic (p,2p)- [2,7] and (π^-,π^-p)- [8] experiments. Information about two-hole excitations of the residual nucleus and the momentum distributions of p-n pairs inside a nucleus has been obtained from the following reactions: (γ,pn) (e.g. ref. 9), (π^-,2n) [10,11], (π^+,2p) [12,13] and (p,pd) [14-18]. Recently preliminary results of a ^{6}Li(e,e'd)-experiment at 0.5 GeV have been published[19].

We now present a short description of the apparatus (Sec. 2), the data analysis and the corrections (Sec. 3), a comparison with theoretical models (Sec. 4.1 and 4.2, for protons and deuterons respectively), and our conclusions are then summarized (Sec. 5).

2. Apparatus

Electrons with a known energy E were scattered from a solid Li-target (alternatively from a liquid H_2- or D_2-target) and detected at an angle Θ_e. Coincident recoil particles (protons and deuterons) were detected by a counter hodoscope. By analysis of the electron momentum and the mass as well as angle and energy of the recoil particles it was possible to determine all other kinematic parameters. The experimental arrangement has been previously described in detail[20-27].

A slowly ejected electron beam was produced by the Deutsches Elektronen-Synchrotron (DESY) with energies of 2.5 GeV or 2.7 GeV and an energy resolution of about ± 0.5 %. The intensity of this incident electron beam was monitored by a secondary emission monitor and a totally absorbing Faraday cup.

The lithium target was a solid plate (95.6 % ^6Li, 4.4 % ^7Li by volume) oriented 45° to the incident beam direction. Thus the effective thickness was (5.7 ±0.3) mm, corresponding to $3.8 \cdot 10^{-3}$ radiation lengths. The target was placed in a scattering chamber with Kapton H windows of 0.125 mm thickness. In addition, dry He-gas continually flowed through the scattering chamber.

The electron spectrometer contained a magnet with a homogeneous field (DESY MB magnet), followed by a series of four wire-spark chambers, three scintillation counters and a shower counter to distinguish electrons from background particles.

The horizontal aperture of the spectrometer was 1.57° resulting in a solid angle acceptance of $0.695 \cdot 10^{-3}$ sr. The momentum acceptance was ±20 % with a mean momentum resolution of ±0.6 %.

The recoil particles were detected by a three plane scintillation counter hodoscope. In the first (second) plane twelve counters, each 432 mm x 36 mm x 10 mm,

were aligned horizontally (vertically). The third plane consisted of four thick quadrant counters, each 216 mm x 216 mm x 50 mm. This counter hodoscope covered an aperture of 31° x 31° which was subdivided by the first two planes into 144 elements, each 2.57° x 2.57°.

The information stored in the spark chamber ferrite core readout system, the digitized counter pulse heights and additional data concerning charge, dead time and accidental coincidences collected in scalers were processed by 100 MHz-electronics and transferred on-line to a CDC-1700 computer. Simultaneously, the proper function of the entire apparatus could be controlled by programs which monitored the spark chamber efficiencies, the counter pulse height spectra and the momentum spectra of scattered electrons.

According to the momentum transfer criteria of section 1 we chose the sets of kinematic parameters listed in table 1. For convenience the corresponding squared four-momentum transfers, scattering and recoil angles and energies of protons and deuterons are presented for the case of elastic e-p- and e-d-scattering.

3. Evaluation of Data

The broadening of the quasi-elastic peak due to the Fermi-momenta of the nucleons made it difficult to separate the deuterons from the large low-energy tail of the protons. Therefore, it was necessary to use a differential method, comparing for every recoil particle its set of pulse heights in the three counter planes with those of calibration energies from the elastic e-p- and e-d-scattering. The total energy loss of particles stopped in the third plane permitted a discrimination between protons and deuterons. Other particles, like tritons and α-particles had

too little energy to be detected. Background particles, such as pions, nucleons and low-energy-electrons were rejected by pulse height discrimination. Low-energy-γ-quanta were absorbed by a 0.5 mm thick lead foil in front of the hodoscope.

The following corrections have been taken into account for every event:

1) Long-time drifts in the counter pulse heights (typically 5 % - 15 %)
2) Light-absorption in the scintillators (max. 7 %)
3) Difference of the light yield from protons and deuterons ("quenching effect")[28]
4) Energy loss in target, air and lead foil
5) The flux variation of the incident electrons due to the Fermi motion of the target particles (typically 5 %)

The whole separation method has been checked experimentally by applying it to measurements of the elastic e-p- and e-d-scattering.

From the comparison with these data we obtained an identification efficiency of about 85 % for protons in the energy range 30 - 330 MeV, and about 65 % for deuterons in the range 45 - 145 MeV, depending slightly on the particle energy.

The total systematic error for the proton cross sections amounts to ±8 %, obtained from quadratic addition of all uncertainties of counter and spark chamber efficiencies. The corresponding systematic error for the deuteron measurements is ±20 %, reflecting the error in the subtraction of "background deuterons" simulated by other particles. Additionally, the error in the absolute cross section scale is ±7 %, arising from target, incident beam, solid angle and dead time uncertainties.

4. Results and Comparison with Theoretical Models

Experimental results for outgoing protons and deuterons are represented in fig. 1 and fig. 2, respectively. All results are tabulated in ref. 29. From the measured fourfold differential cross sections we obtained by integration over two variables within the range of experimentally accessible angles and energies the following double differential cross sections:

a) $\frac{d^2\sigma}{d\Omega_e\, dE'}$ b) $\frac{d^2\sigma}{d\Omega_e\, dE_i}$ c) $\frac{d^2\sigma}{d\Omega_e\, d\Omega_i}$

where E', Ω_e refer to the scattered electrons and
E_i, Ω_i $(i = p,d)$ refer to the recoil protons and deuterons.

d) In addition, we have calculated the distribution $P(q_R)$ of the recoil nucleus momenta q_R including the phase space factor q_R^{-2},
where $\vec{q}_R = \vec{q} - \vec{k}_i$ is the "missing" momentum of the recoil nucleus,
$\vec{q}$ is the three momentum transfer and
$\vec{k}_i$ $(i = p,d)$ are the momenta of the recoiling particles.

The error bars in figs. 1 and 2 include both the statistical and the systematic errors. The energy, angular and momentum resolutions have been determined experimentally (by elastic e-p- and e-d-scattering) and are given by the dotted curves in figs. 1 and 2. The largest contributions to the resolution result from the angular aperture of the electron spectrometer and from the energy width of the incident beam. The arrows give the calculated position of the free e-p- and e-d-scattering, respectively.

Because it was not possible to perform radiative corrections by "unfolding" our experimental spectra, we used the inverse method. Starting from theoretical Fer-

mi-momentum distributions we calculated threefold differential cross sections[30]. By applying the inverse of the usual radiative corrections[31] to the threefold differential cross sections and then integrating, we were able to obtain a theoretical "radiated" double-differential cross section which could then be compared with our uncorrected experimental points. A similar procedure was used to calculate a momentum distribution to be compared with $P(q_R)$. The corresponding double-differential cross sections with the radiative effects not included (which will be used in sec. 4.2. in comparison with elastic e-d-scattering) were also calculated for those "radiated" cross sections which give a best fit to the data (dashed curves in figs. 1 and 2).

4.1. Quasielastic Scattering with Outgoing Protons

A possibility to analyse the data is given by the Jastrow model of short range correlations. In fig. 1 the proton data are compared with shell-model calculations which include short-range nucleon-nucleon correlations[32], where a Woods-Saxon potential was used. The parameters were obtained from elastic electron-nucleus scattering. The binding energy in the s-shell was assumed to be 22.7 MeV, in the p-shell 4.7 MeV[33]. The correlation is parametrized by q_c, representing the exchanged momentum between otherwise independently moving nucleons. Although there is no strong dependence on the parameter q_c, the best agreement is obtained using $q_c \sim 300$ MeV/c, yielding a χ^2 per degree of freedom of about 1. This value of q_c coincides with those used in calculations of the absorption rate of pions in ^{16}O and the $^6Li(\gamma,p)$ reaction[34,35]. The effect of the short-range nucleon-nucleon correlations is illustrated in fig. 3: If we admit correlations with $q_c = 300$ MeV/c, the theoretical momentum distribution $P(q_R) \cdot q_R^2$ is increased for $q_R \gtrsim 200$ MeV/c and yields better agreement with the experiment.

Although we were not able to separate the s- and p-shells of ^{6}Li, the parameters of the momentum distributions used here (105 MeV/c at 1/e of the maximum for the s-shell and 71 MeV/c for the half-distance between the p-shell maxima) are in very good agreement with the (e,e'p)-date of Antoufiev et al.[5] at 1.18 GeV and of Hiramatsu et al.[6] at 700 MeV. Earlier measurements of (p,2p)-quasi-elastic scattering[7] yield a comparable s-shell parameter, but yield for the p-shell parameter a value of $\sim$ 40 MeV/c.

If we assume the plane wave impulse approximation, i. e. no distortion of the initial and final electron and proton waves, it is justified to equate the "missing momentum" q_R with the negative value of the Fermi-momentum of the moving target nucleon. Calculations for the even heavier nucleus ^{12}C show that for outgoing proton energies $\gtrsim$ 100 MeV the shapes of the distributions are only slightly changed by final state interaction in the region of high momenta ($q_R \gtrsim$ 200 MeV/c) [30] and that mainly a cross section reduction occurs[36]. This final state absorption can be characterized by a nuclear "transparency" for outgoing protons as shown in fig. 4. The experimental points are obtained by dividing the number of proton coincidences by the proton contribution to the quasi-elastic peak found in the single arm events[29]. This proton contribution to the peak was calculated using the Rosenbluth formula with scaling law, dipole fit and $G_{EN} = 0$. The results are compatible with optical-model calculations of Jacob and Maris[37] and following de Carvalho et al.[38], using total nucleon-nucleon cross sections of 23.5 - 29 mb.

Another indication of the decrease in final state interactions with increasing proton energy is given by the number of true (e,e'2p)-events as determined in the present experiment. The ratio between the number of two-proton and one-proton events decreases from $(9.0 \pm 0.5) \cdot 10^{-3}$ at $E_p = 138$ MeV to $(6.5 \pm 0.5) \cdot 10^{-3}$ at $E_p = 241$ MeV.

4.2. Scattering with Emission of Deuterons

The emission of deuterons from ^{6}Li in the kinematic region of quasi-elastic scattering has usually been described by a cluster-configuration (α+d) for the ^{6}Li-ground state[39]. The corresponding wave function can be written[40]:

$$\psi_{^6\mathrm{Li}} = \Phi_\alpha(x_\alpha) \cdot \Phi_d(x_d) \cdot \Phi(r)$$

with Φ_α, Φ_d internal α and d wave functions,

$\Phi(r)$ wave function of the relative motion.

Assuming Gaussian shapes for Φ_α, Φ_d and Φ and using parameters obtained from Coulomb scattering, a ground state momentum distribution[41] results:

$$\rho(q) \sim \left| \sum_{i=0,1,2} (a_i + b_i\, q^2)\, e^{-c_i\, q^2} \right|^2$$

with $a_o = -7.500\ \mathrm{fm}^{3/2}$ $b_o = 10.900\ \mathrm{fm}^{7/2}$ $c_o = 2.170\ \mathrm{fm}^2$

$a_1 = 2.360\ \mathrm{fm}^{3/2}$ $b_1 = -0.239\ \mathrm{fm}^{7/2}$ $c_1 = 1.050\ \mathrm{fm}^2$

$a_2 = -1.449\ \mathrm{fm}^{3/2}$ $b_2 = 0.534\ \mathrm{fm}^{7/2}$ $c_2 = 1.073\ \mathrm{fm}^2$.

In addition to the process ^{6}Li(e,e'd) ^{4}He(g.s.), (interpreted as emission from the p-shell), we were able to detect a possible emission of two s-shell nucleons leaving excitations of the residual nuclear system up to $\sim$ 80 MeV, because our cut in the total energy spectrum is 70 - 80 MeV below the peak maximum. In the simplest case, the combination of two s-shell nucleons in a harmonic oscillator potential yields a momentum distribution of Gaussian shape. We chose a width of 210 MeV/c FWHM[9,18] for this distribution, a separation energy of 1.47 MeV for deuterons from the p-shell, and if two s-shell nucleons are emitted, an excitation energy of the residual nucleus of 30 MeV [11]. Having included the experimental cuts in angles and energies, we obtained the best agreement with the data by assuming the ratio for the

number of deuterons for ^{4}He left in the ground state compared to the number of deuterons when the nucleus is left in any possible excited state up to ~ 80 MeV is 1 : 1.1 at 10.4 fm^{-2} (fig. 2). This ratio also has the value 1 : 1.1 at 12.2 fm^{-2} in contrast to 1 : 0.9 at 6.8 fm^{-2}.

Optical model calculations for deuterons with outgoing energies ~ 40 MeV have shown that it is justified to use the plane wave impulse approximation and to neglect the final state distortion effects as we have done in our calculations of the shapes of the distributions displayed in fig. 2[42].

In fig. 5 the effective number of deuterons emitted from ^{6}Li is presented:

$$N_d = \frac{\frac{d\sigma_d}{d\Omega_e}(^6\text{Li})}{\frac{d\sigma_d}{d\Omega_e}(D_2)}$$

where $\frac{d\sigma_d}{d\Omega_e}(^6\text{Li})$ is the integrated double differential cross section for quasi-elastic emission of deuterons from ^{6}Li (see end of sec. 4.), corrected for experimental cuts, and

$\frac{d\sigma_d}{d\Omega_e}(D_2)$ is the well known elastic e-d scattering cross section[25,43].

The errors in fig. 5 are mainly systematic, but also include errors due to the experimental cuts.

The result is a nearly q^2-independent value of $N_d \sim 2$ for excitations up to ~ 80 MeV, enclosed by the cluster-model predictions of Kudeyarow et al.[40]. In the lower limit (g.s. of the residual nucleus), the number of effective deuteron clusters should be 1.1, in the upper limit (g.s. plus all excitations of the residual nucleus)

this value was predicted to be 4.2. An alternative description by Jeremie[44] calculates the probability for two nuclear nucleons in shell model states to be scattered like a free deuteron. This is a special way of introducing nucleon-nucleon correlations. The final-state absorption is included by an eikonal approximation with the real part of the potential set equal to 65 MeV and the imaginary part, W_o, set equal to 10 MeV or 12.5 MeV. Although the precision of the data does not allow to distinguish between these values of W_o, it is clear that the theoretical predictions are in very good agreement with the experimental data.

Fig. 6 gives the ratio of the number of emitted deuterons to that of the emitted protons, depending on the square of the four-momentum transfer, $-q^2$. The curves represent the published data[25,43] for the form factors squared,

$$G_p^2(q^2) = \frac{\left(\frac{d\sigma}{d\Omega}\right)_{e-p}}{\left(\frac{d\sigma}{d\Omega}\right)_{Mott}} \quad \text{(for protons);} \qquad G_d^2(q^2) = \frac{\left(\frac{d\sigma}{d\Omega}\right)_{e-d}}{\left(\frac{d\sigma}{d\Omega}\right)_{Mott}} \quad \text{(for deuterons)}$$

and their ratio $G_d^2(q^2)/G_p^2(q^2)$ for $\theta_e = 13.8^o$. The experimental points,

$$R = \left(\frac{d\sigma_d}{d\Omega_e} (^6Li) \Big/ \frac{d\sigma_p}{d\Omega_e} (^6Li) \right) \cdot \frac{\tilde{N}_p \cdot D_p}{\tilde{N}_d \cdot D_d}$$

are obtained from the measured rates for deuteron and proton emission from ^6Li, the effective numbers of target particles per nucleus, $\tilde{N}_i$, and the final-state transparencies, D_i. ($\tilde{N}_p = 3$, D_p is taken from fig. 4, $N_d = \tilde{N}_d \cdot D_d$ from fig. 5).

The agreement of the experimental deuteron to proton ratios with the curve $G_d^2(q^2)/G_p^2(q^2)$ illustrates that the "form factor" for the emission of deuterons from ^6Li has essentially the same q^2-dependence as the form factor for elastic e-d-scattering. This interpretation of figs. 5 and 6 assumes a nearly constant

final-state absorption of the deuterons in the energy range of this experiment.

The widths of the deuteron momentum distributions and the effective numbers of deuterons for the ground-state process and excitations of the residual nucleus are presented in addition to comparisons with other reactions in table 2. The distribution used for the (e,e'd) ^{4}He(g.s)-part of our data has also been used for description of the (p,pd)-data of Alder et al. at 590 MeV. It exhibits sufficient agreement with the (α,2α)-data at 104 MeV and excellent agreement with both (π^-,nn)-experiments and the (π^+,pp)-data at 76 MeV.

The (p,pd)-data at energies $\leq$ 155 MeV and the preliminary (e,e'd)-data at 515 MeV show smaller widths. This difference is presumably due to the strong absorption of the outgoing low-energy deuterons, and additionally in the (p,pd)-case, due to the distortion of the incoming and outgoing proton waves. The value of 210 MeV/c, used in our calculation of the distribution with excited residual nuclei, agrees well with the result of $\sim$ 226 MeV/c obtained in the (π^-,nn)-experiment of Calligaris et al.

The value of N_d determined by this experiment, which includes excitations up to $\sim$ 80 MeV, agrees within the errors with all (π^+,pp)-data and the (p,pd)-measurement at 590 MeV (energy of the outgoing deuterons $\sim$ 210 MeV), in spite of the different reaction mechanism. The values obtained from (p,pd)-measurements at 670 and 1000 MeV are larger than our values, perhaps because the outgoing deuterons with energies of $\sim$ 580 MeV and $\sim$ 900 MeV, respectively, are less affected by final-state absorption.

5. Conclusions

We summarize the results of the quasi-elastic scattering process ^{6}Li(e,e'p) as follows:

1) As expected, the spectra of the scattered electrons and protons and the angular distributions show a broadening due to the Fermi motion of the nucleons in the initial ^{6}Li-nucleus and a shift of the peak maximum due to the nucleon binding energy.

2) These data are well described by shell-model wave functions that include short range nucleon-nucleon correlations. Although no definite conclusion can be drawn, a better agreement with the data for Fermi-momenta $q_R \geq 200$ MeV/c is obtained if the correlations are described by a momentum exchange between the nucleons of $q_c \sim 300$ MeV/c.

3) With increasing energy of the outgoing protons, the nuclear transparency increases and the probability for the emission of two nucleons decreases, reflecting the influence of final-state interactions.

For the process ^{6}Li(e,e'd), the energy spectra of the scattered electrons and deuterons, the deuteron angular distribution, and the momentum distribution of the residual nuclei can all be consistently described as follows:

1) Cluster-wave functions for the p-shell nucleons and harmonic-oscillator wave functions for the s-shell nucleons with relative weights of about 1 : 1 yield the best fit.

2) The effective number of deuterons, given by the cross section for quasi-elastic emission of deuterons from ^{6}Li, divided by the elastic electron-deuteron scattering cross section, turns out to be about 2, independent of the square of the four momentum transfer. The effective number of deuterons estimated by Jeremie[44] is in good agreement with the experiment.

3) Because the effective number of deuterons is essentially constant, we can also conclude that the "form factor" for the quasi-elastic emission of deuterons from ^{6}Li shows the same q^2-dependence as the elastic electron-deuteron scattering from factor.

Acknowledgments

We are indebted to the directors of our institutions for their constant interest in this work. Interesting discussions with Prof. M.G. Huber, Dr. W. Weise, Dr. P.G. Reinhardt and Dr. H. Jeremie are gratefully acknowledged. We thank the staff of DESY for their support during the runs and specially Ing. H. Sindt for his excellent assistance in all stages of the experiment.

This work has been supported by the Bundesministerium für Forschung und Technologie.

Figure Captions

Fig. 1 Proton coincidence data at $E = 2.7$ GeV, $\Theta_e = 13.8^\circ$.

a) Double-differential cross section as a function of the energy of scattered electons.

b) Double-differential cross section as a function of the proton energy.

c) Proton angular distribution. The area enclosed by the experimental points is normalized to 1.

d) Momentum distribution $P(q_R)$ of the residual nucleus, computed using the data a) - c), normalized to 0.95 at 20 MeV/c. In the impulse approximation, this distribution is identical with the Fermi-momentum distribution of the nuclear protons.

Fig. 2 Deuteron coincidence data at $E = 2.7$ GeV, $\Theta_e = 13.8^\circ$. Parts a) - d) as in Fig. 1, replacing protons by deuterons. The curve d) is normalized to 1 at 0 MeV/c.

Fig. 3 Momentum distribution $P(q_R) \cdot q_R^2$ of the residual nucleus at $E = 2.7$ GeV, $\Theta_e = 13.8^\circ$ (cf. Fig. 1d).
The curves represent a pure shell-model calculation and a wave function including correlations with a momentum exchange $q_c = 300$ MeV/c (Blum[32]). The effects of radiation and experimental cuts are included in the theoretical curves.

Fig. 4 Transparency for protons from the reaction $^{6}Li(e,e'p)$ as a function of the proton energy. The curves are calculations using an optical model.

Fig. 5 The effective number of deuterons N_d, defined as ratio of the deuteron emission differential cross section from ^{6}Li to the elastic e-d scattering differential cross section, as a function of the square of the four momentum transfer. For comparison, a result from the best fit to the spectra (fig. 2) and various theoretical models are presented.

Fig. 6 Ratio R of the detected deuterons to the detected protons, corrected for the effective numbers of deuteron and proton target particles and for the final-state transparencies. The curve labeled G_d^2/G_p^2 is a best fit to the published data for free deuterons and protons.

References

1) M.G. Huber, Annales de Physique 5 (1970) 239

2) G. Jacob, Th.A.J. Maris, Rev. Mod. Phys. 38 (1966) 121

3) U. Amaldi jr., Suppl. Nuovo Cimento Ser. I, 5 (1967) 1225

4) A. Malecki, P. Picchi, Riv. Nuovo Cimento II (1970) 119

5) Yu.P. Antoufiev, V.L. Agranovich, V.S. Kuzmenko, P.V. Sorokin, Physics Letters 42B (1972) 347

6) H. Hiramatsu, T. Kamae, H. Muramatsu, K. Nakamura, N. Izutsu, Y. Watase, Physics Letters 44B (1973) 50

7) M. Riou, Rev. Mod. Phys. 37 (1965) 375

T. Berggren, H. Tyrén, "Quasi-free Scattering" in: Annual Review of Nuclear Science (Ed. by E. Segrè, G. Friedlander, H.P. Noyes) Vol. 16 (1966) p. 153

8) Yu.D. Bayukov, L.S. Vorobyev, V.M. Kolybasov, G.A. Leksin, V.L. Stolin, V.B. Fedorov, V.D. Khovansky, Yadern. Fiz. 17 (1973) 916

9) B. Mecking, Thesis Bonn 1972 and UNIV BONN PIB 1-155 (1972)

10) H. Davies, H. Muirhead, J.N. Woulds, Nucl. Phys. 78 (1966) 663

11) F. Calligaris, C. Cernigoi, I. Gabrielli, F. Pellegrini, Nucl. Phys. A126 (1969) 209

12) G. Charpak, G. Gregoire, L. Massonnet, J. Saudinos, J. Favier, M. Gusakow, M. Jean, Physics Letters 16 (1965) 54

G. Charpak, J. Favier, L. Massonnet, C. Zupancic, in: International Nuclear Physics Conference, Gatlinburg, Tennessee, September 12 - 17, 1966 (Ed. by R.L. Becker, New York and London 1967, p. 465)

13) T. Bressani, G. Charpak, J. Favier, L. Massonnet, W.E. Meyerhof, C. Zupancic, Nucl. Phys. B9 (1969) 427

14) D.W. Devins, B.L. Scott, H.H. Forster, Rev. Mod. Phys. 37 (1965) 396

15) C. Ruhla, M. Riou, J.P. Garron, J.C. Jacmart, L. Massonnet, Physics Letters 2 (1962) 44

C. Ruhla, M. Riou, M. Gusakow, J.C. Jacmart, M. Liu, L. Valentin, Physics Letters 6 (1963) 282

16) J.C. Alder, W. Dollhopf, W. Kossler, C.F. Perdrisat, W.K. Roberts, P. Kitching, G.A. Moss, W.C. Olsen, J.R. Priest, Phys. Rev. C6 (1972) 18

17) L.S. Azhgirei, Z. Cisek, O.D. Dalkarov, Z.V. Krumshtein, Yu.P. Merekov, Z. Moroz, Ngo Quang Ziu, V.I. Petrukhin, A.I. Ronzhin, G.A. Shelkov, DUBNA JINR-P-1-6308 (1972)

18) R.J. Sutter, J.L. Friedes, H. Palevsky, G.W. Bennett, G.J. Igo, W.D. Simpson, G.C. Phillips, D.M. Corley, N.S. Wall, R.L. Stearns, Phys. Rev. Letters 19 (1967) 1189

19) J.P. Génin, J.Julien, R. Letourneau, A. Mougeot, J. Rambaut, C. Samour, in: Proc. of the International Conference on Nuclear Structure Studies Using Electron Scattering and Photoreaction, Sendai, 12-15 Sept. 1972, p. 439, and J. Julien, C. Samour, G. Bianchi, P. Duval, J.P. Génin, R. Letourneau, A. Mougeot, M. Rambaut, Contributed Papers to the Fifth Int. Conference on High Energy Physics and Nuclear Structure, Uppsala, June 18 - 22, 1973, p. 171

20) S. Galster, J. Görres, G. Hartwig, H. Klein, J. Moritz, W. Schmidt-Parzefall, H. Schopper, Nucl. Instr. Meth. 46 (1967) 208

21) W. Schmidt- Parzefall, KFK-Report 769 (1968)

22) S. Galster, G. Hartwig, H. Klein, J. Moritz, K.H. Schmidt, W. Schmidt-Parzefall, H. Schopper, D. Wegener, Nucl. Instr. Meth. 76 (1969) 337

23) S. Galster, G. Hartwig, H. Klein, J. Moritz, K.H. Schmidt, W. Schmidt-Parzefall, D. Wegener, J. Bleckwenn, KFK-Report 963 (1969)

24) H. Klein, Thesis Karlsruhe 1970

25) K.H. Schmidt, Thesis Karlsruhe 1970 and Internal Report DESY F23-70/1 (1970)

26) J. Moritz, Thesis Karlsruhe 1970 and Internal Report DESY F23-71/1 (1971)

S. Galster, G. Hartwig, H. Klein, J. Moritz, K.H. Schmidt, W. Schmidt-Parzefall, D. Wegener, J. Bleckwenn, DESY Report 71/44 (1971 and Phys. Rev. D5 (1972) 519

27) J. Bleckwenn, Thesis Karlsruhe 1971 and Internal Report DESY F23-71/2 (1971)

J. Bleckwenn, H. Klein, J. Moritz, K.H. Schmidt, D. Wegener, Nucl. Phys. B33 (1971) 475

28) G.T. Wright, Phys. Rev. 91 (1953) 1282

T.J. Gooding, H.G. Pugh, Nucl. Instr. Method. 7 (1960) 189

29) F.H. Heimlich, Thesis Freiburg/Brsg. 1973 and Internal Report DESY F23-73/1 (1973)

30) W. Weise, Nucl. Phys. A 193 (1972) 625

V. Devanathan, Ann. Phys. 43 (1967) 74

31) L.W. Mo, Y.S. Tsai, Rev. Mod. Phys. 41 (1969) 205

32) B. Blum, Thesis Erlangen-Nürnberg 1972

B. Blum, M.G. Huber, to be published

33) L.R.B. Elton, A. Swift, Nucl. Phys. A94 (1967) 52

34) K. Chung, M. Danos, M.G. Huber, Physics Letters 29B (1969) 265

35) W. Weise, Physics Letters 38B (1972) 301

36) C.D. Epp, T.A. Griffy, Phys. Rev. C1 (1970) 1633

37) G. Jacob, Th.A.J. Maris, Nucl. Phys. 31 (1962) 139

38) H.G. de Carvalho, J.B. Martins, O.A.P. Tavares, R.A.M.S. Nazareth, V. di Napoli, Notas de Física XVII (1971) 217

39) K. Wildermuth, W. McClure, Springer Tracts in Modern Physics, Vol. 41 (1966)

40) Yu.A. Kudeyarov, I.V. Kurdyumov, V.G. Neudatchin, Yu.F. Smirnov, Nucl. Phys. A163 (1971) 316

41) I.V. Kurdyumov, Thesis Moskau 1971

V.G. Neudatchin, private communication

42) T.A. Griffy, R.J. Oakes, H.M. Schwartz, Nucl. Phys. 86 (1966) 313

43) S. Galster, H. Klein, J. Moritz, K.H. Schmidt, D. Wegener, J. Bleckwenn, Nucl. Phys. B23 (1971) 221

44) H. Jérémie, Physics Letters 40B (1972) 311

45) E. Velten, Thesis Karlsruhe 1969

46) A. Bussière, A. Gillebert, J. Mougey, Phan Xuan Ho, M. Priou, D. Royer, I. Sick, Contributed Papers to the Fifth Int. Conference on High Energy Physics and Nuclear Structure, Uppsala, June 18 - 22, 1973, p. 170

47) F.H. Heimlich, E. Rössle, M. Köbberling, J. Moritz, K.H. Schmidt, D. Wegener, D. Zeller, J.K. Bienlein, J. Bleckwenn, H. Dinter, DESY-Report 71/55 (1971) and Proc. of the Int. Conference on Photonuclear Reactions and Applications, Asilomar (Calif.) 1973, p. 8 A6

Table 1 Kinematic parameters

Incident electron energy E	Electron scattering angle Θ_e	Square of the four-momentum transfer $-q^2$	Energy of scattered electrons E'	Protons: Recoil proton angle Θ_p	Protons: Recoil proton energy E_p
2.5 GeV	12 ^{o}	6.6 fm^{-2} 0.26 $(GeV/c)^2$	2.36 GeV	68.9^o	138 MeV
2.7 GeV	13.8^o	10.0 fm^{-2} 0.39 $(GeV/c)^2$	2.49 GeV	64.9^o	207 MeV
2.7 GeV	15 ^{o}	11.6 fm^{-2} 0.45 $(GeV/c)^2$	2.46 GeV	63.0^o	241 MeV

Incident electron energy E	Electron scattering angle Θ_e	Square of the four-momentum transfer $-q^2$	Energy of scattered electrons E'	Deuterons: Recoil deuteron angle Θ_d	Deuterons: Recoil deuteron energy E_d
2.5 GeV	12 ^{o}	6.8 fm^{-2} 0.27 $(GeV/c)^2$	2.43 GeV	76.2^o	71 MeV
2.7 GeV	13.8^o	10.4 fm^{-2} 0.40 $(GeV/c)^2$	2.59 GeV	73.6^o	108 MeV
2.7 GeV	15 ^{o}	12.2 fm^{-2} 0.47 $(GeV/c)^2$	2.57 GeV	72.2^o	126 MeV

The values of $-q^2$, E', $\Theta_{p,d}$ and $E_{p,d}$ refer to the elastic electron-proton and the elastic electron-deuteron scattering, respectively.

Table 2 Two-Nucleon emission from ^{6}Li

Reaction	Primary energy (MeV)	FWHM for ^{4}He(g.s.) (MeV/c)	FWHM for ^{4}He(~30 MeV) (MeV/c)	N_d(g.s.)	N_d(g.s. + excitations)	N_d(g.s.): N_d(exc.)	References	
$^{6}Li(p,pd)$	30.5	66 ±17		0.07			D.W. Devins et al.	(14)
	155	63		0.31 ±0.15			C. Ruhla et al.	(15)
	590	124 ± 4		0.80 ±0.06	~1.5*	1 : 0.85*	J.C. Alder et al.	(16)
	670				3.62 ±0.15		L.S. Azhgirei et al.	(17)
	1000				~3.2		R.J. Sutter et al.	(18)
$^{6}Li(\alpha,2\alpha)$	104	73-113					E. Velten	(45)
$^{6}Li(\pi^-,nn)$	at rest	~120		0.37 ±0.10			H. Davies et al.	(10)
	at rest	~126	~226			1 : 1.3**	F. Calligaris et al.	(11)
$^{6}Li(\pi^+,pp)$	76	~125		0.4	1.2*	1 : 2*	G. Charpak et al.	(12)
	51-272			0.8-1.1	1.3-1.7***	1 : 1.5***	T. Bressani et al.	(13)
$^{6}Li(e,e'd)$	515	~60					J.P. Genin et al.	(19)
	2500	124	210		1.9 ±0.6*	1 : 0.9*	this work	
	2700	124	210		2.1 ±0.7*	1 : 1.1*	this work	
					2.2 ±1.0*	1 : 1.1*	this work	

* excitations up to 80 MeV
** up to 70 MeV
*** up to 50 MeV

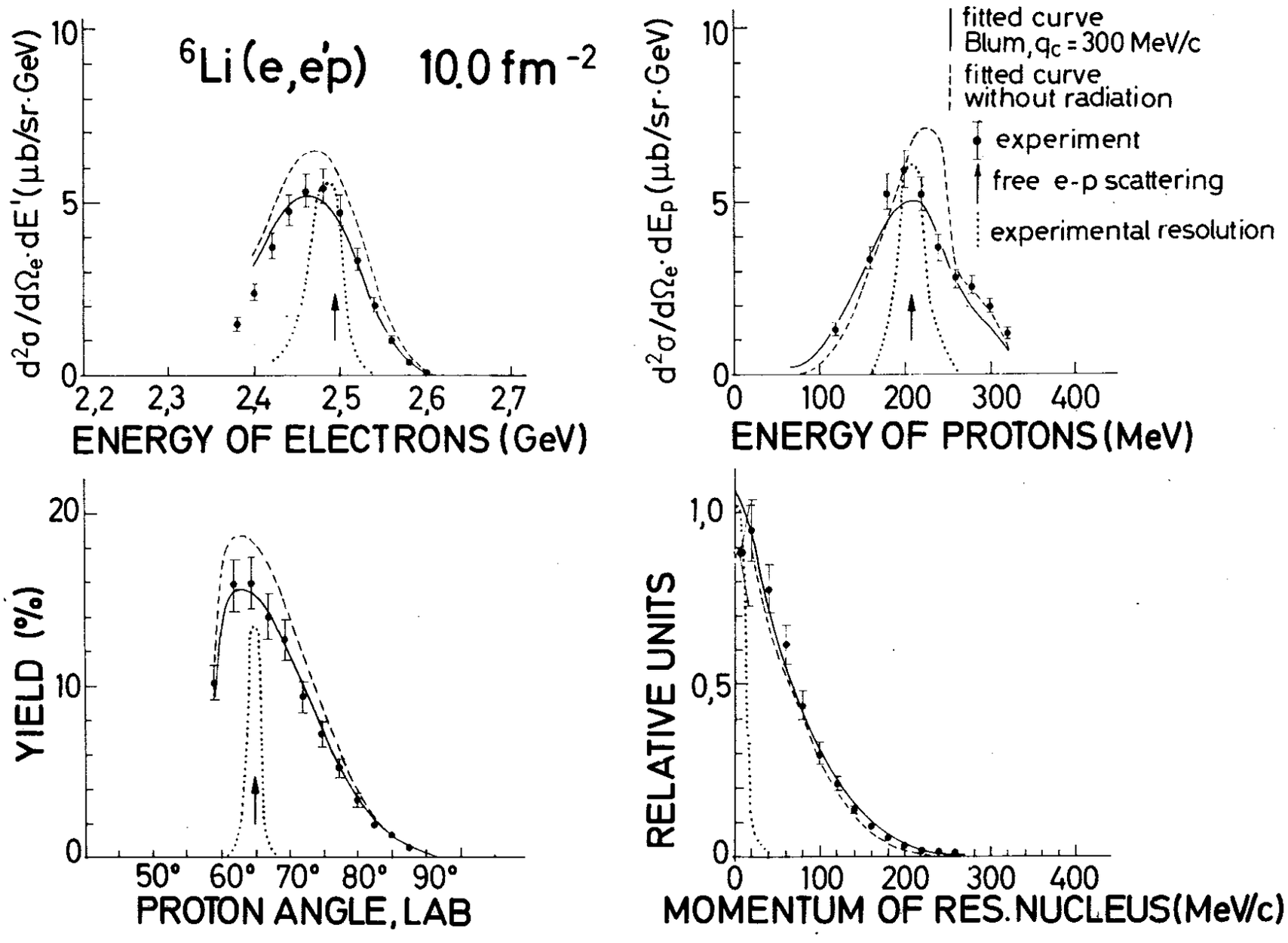
^{6}Li (e,e'p) 10.0 fm^{-2}
$d^2\sigma/d\Omega_e \cdot dE'$ (μb/sr·GeV)
ENERGY OF ELECTRONS (GeV)
fitted curve
Blum, q_c = 300 MeV/c
fitted curve
without radiation
experiment
free e-p scattering
experimental resolution
$d^2\sigma/d\Omega_e \cdot dE_p$ (μb/sr·GeV)
ENERGY OF PROTONS (MeV)
YIELD (%)
PROTON ANGLE, LAB
RELATIVE UNITS
MOMENTUM OF RES. NUCLEUS (MeV/c)

FIG. 1

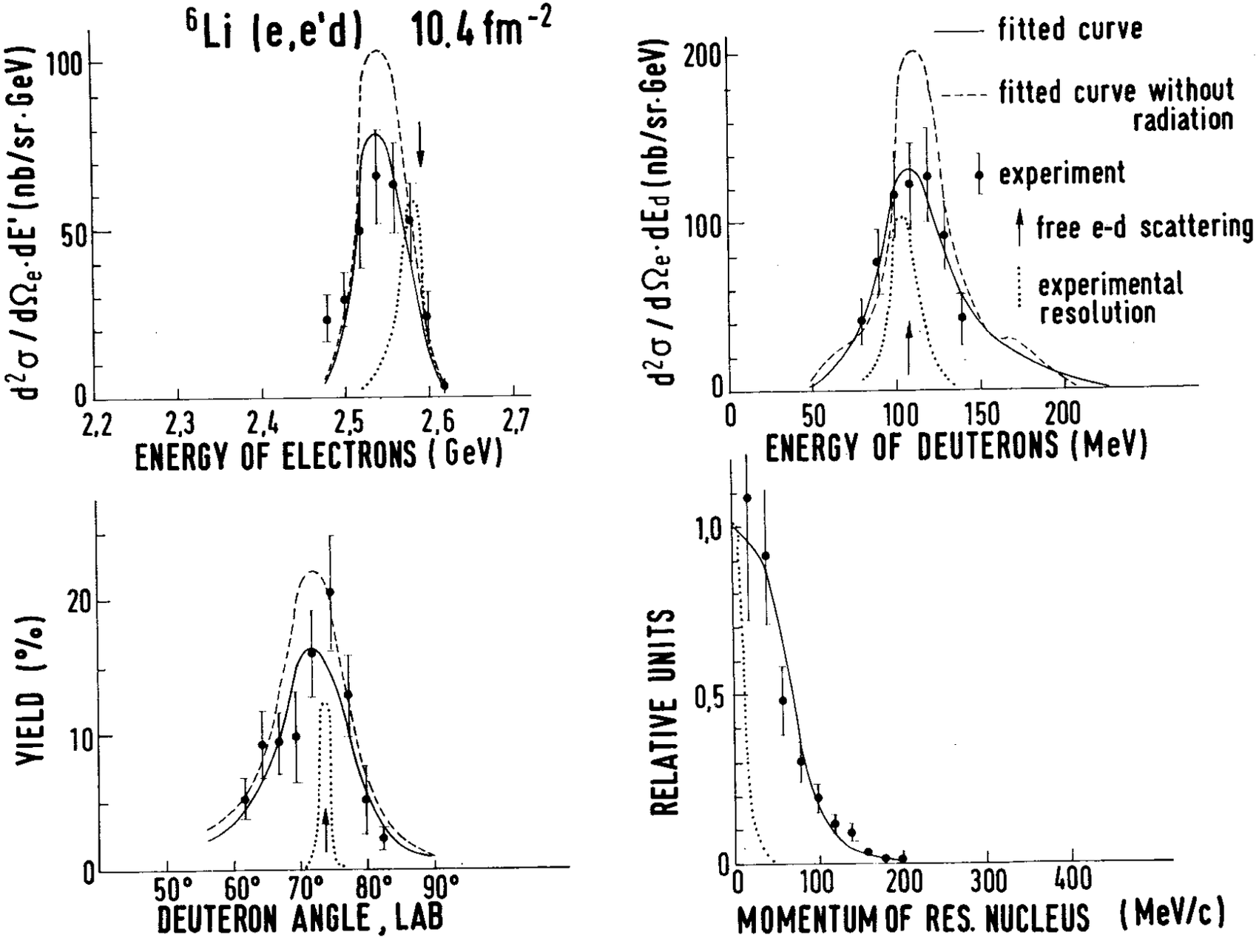
^{6}Li (e,e'd) 10.4 fm^{-2}
$d^2\sigma / d\Omega_e \cdot dE'$ (nb/sr·GeV)
100
50
0
2,2
2,3
2,4
2,5
2,6
2,7
ENERGY OF ELECTRONS (GeV)
fitted curve
fitted curve without radiation
experiment
free e-d scattering
experimental resolution
$d^2\sigma / d\Omega_e \cdot dE_d$ (nb/sr·GeV)
200
100
0
50
100
150
200
ENERGY OF DEUTERONS (MeV)
YIELD (%)
20
10
0
50°
60°
70°
80°
90°
DEUTERON ANGLE, LAB
RELATIVE UNITS
1,0
0,5
0
100
200
300
400
MOMENTUM OF RES. NUCLEUS (MeV/c)

FIG.2

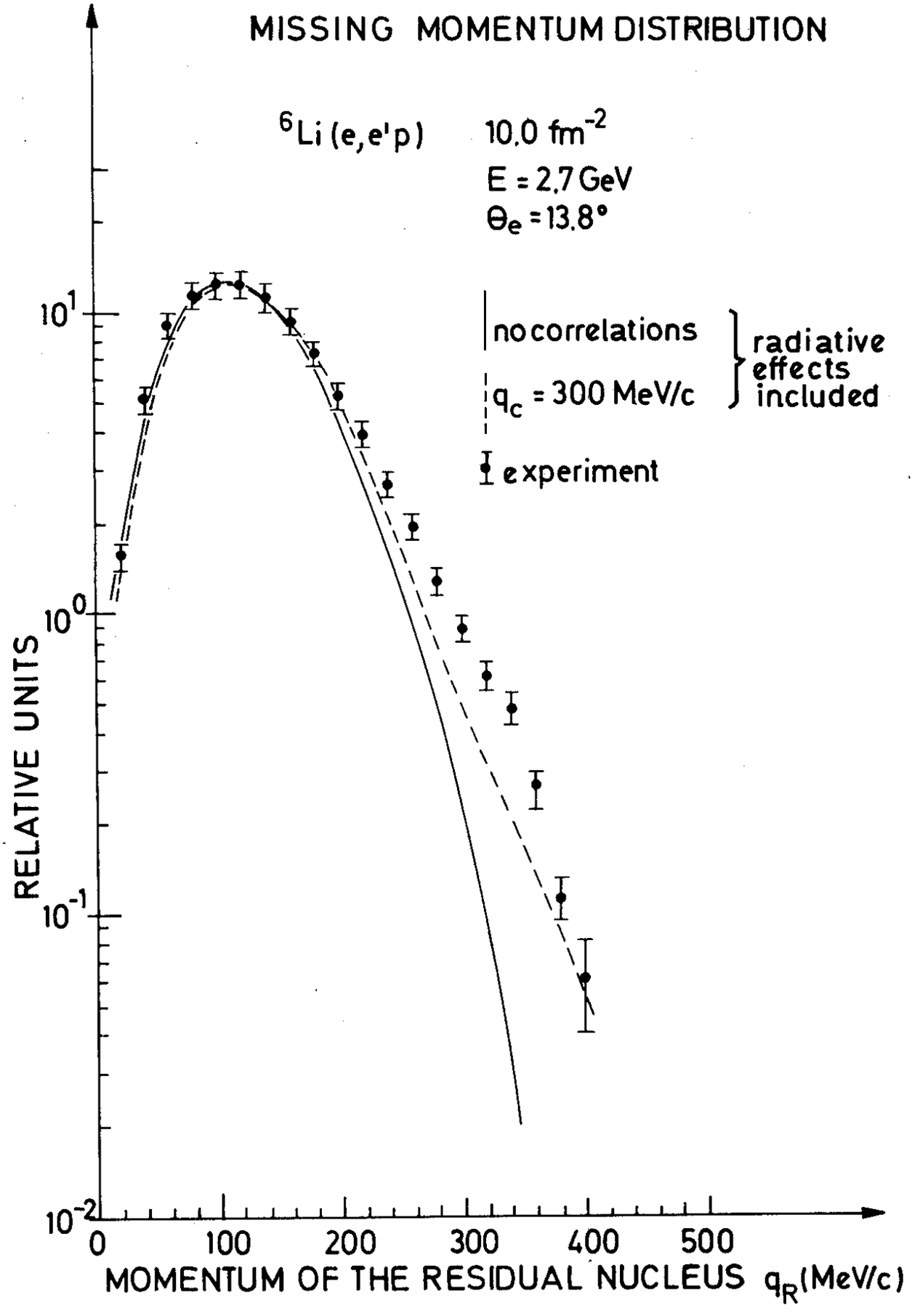
MISSING MOMENTUM DISTRIBUTION
^{6}Li (e,e'p)
10.0 fm^{-2}
E = 2.7 GeV
Θ_e = 13.8°
no correlations
q_c = 300 MeV/c
radiative effects included
experiment
RELATIVE UNITS
10^1
10^0
10^{-1}
10^{-2}
0
100
200
300
400
500
MOMENTUM OF THE RESIDUAL NUCLEUS q_R(MeV/c)

FIG.3

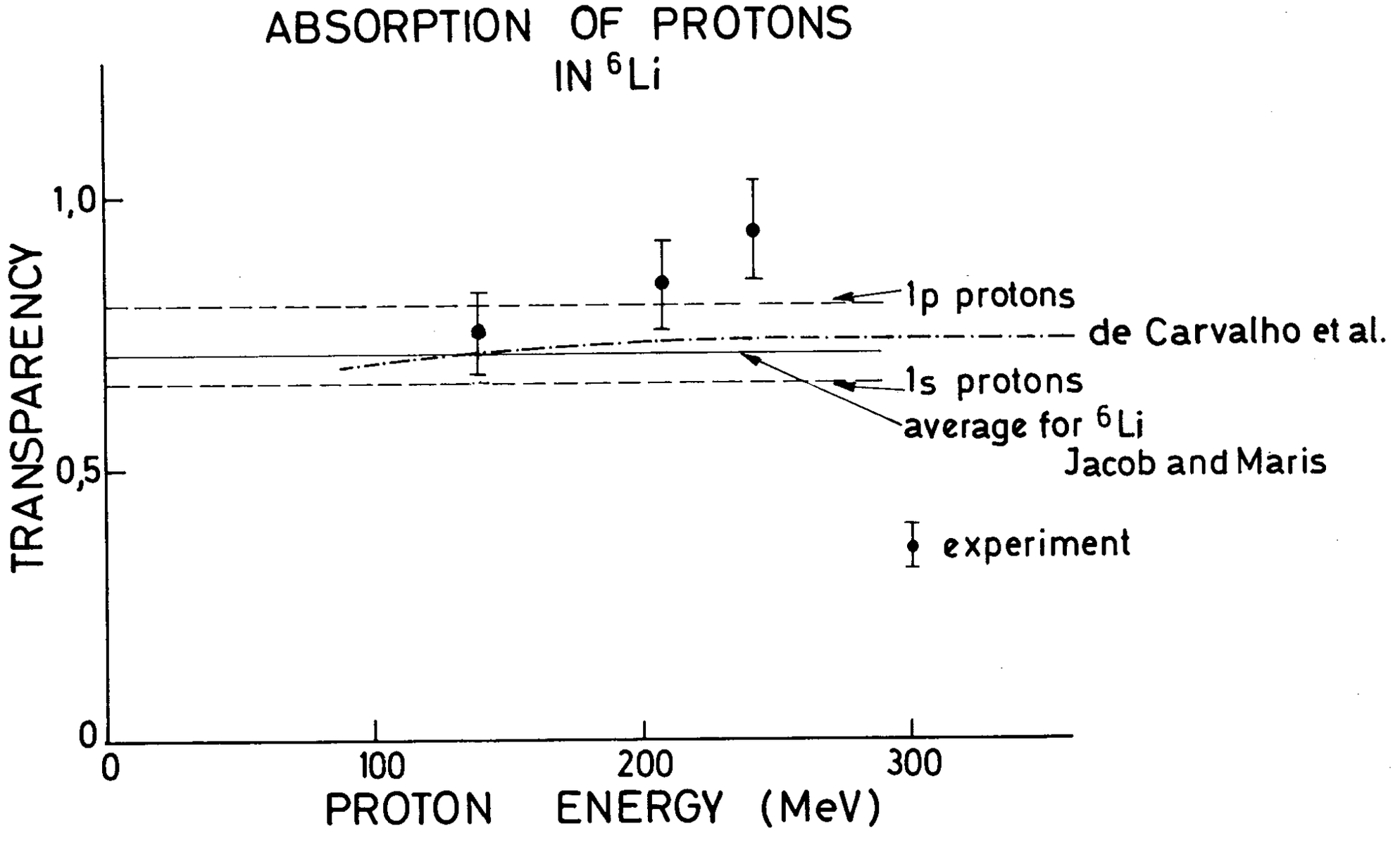
ABSORPTION OF PROTONS
IN ^{6}Li
TRANSPARENCY
1,0
0,5
0
0
100
200
300
PROTON ENERGY (MeV)
1p protons
de Carvalho et al.
1s protons
average for ^{6}Li
Jacob and Maris
experiment

FIG.4

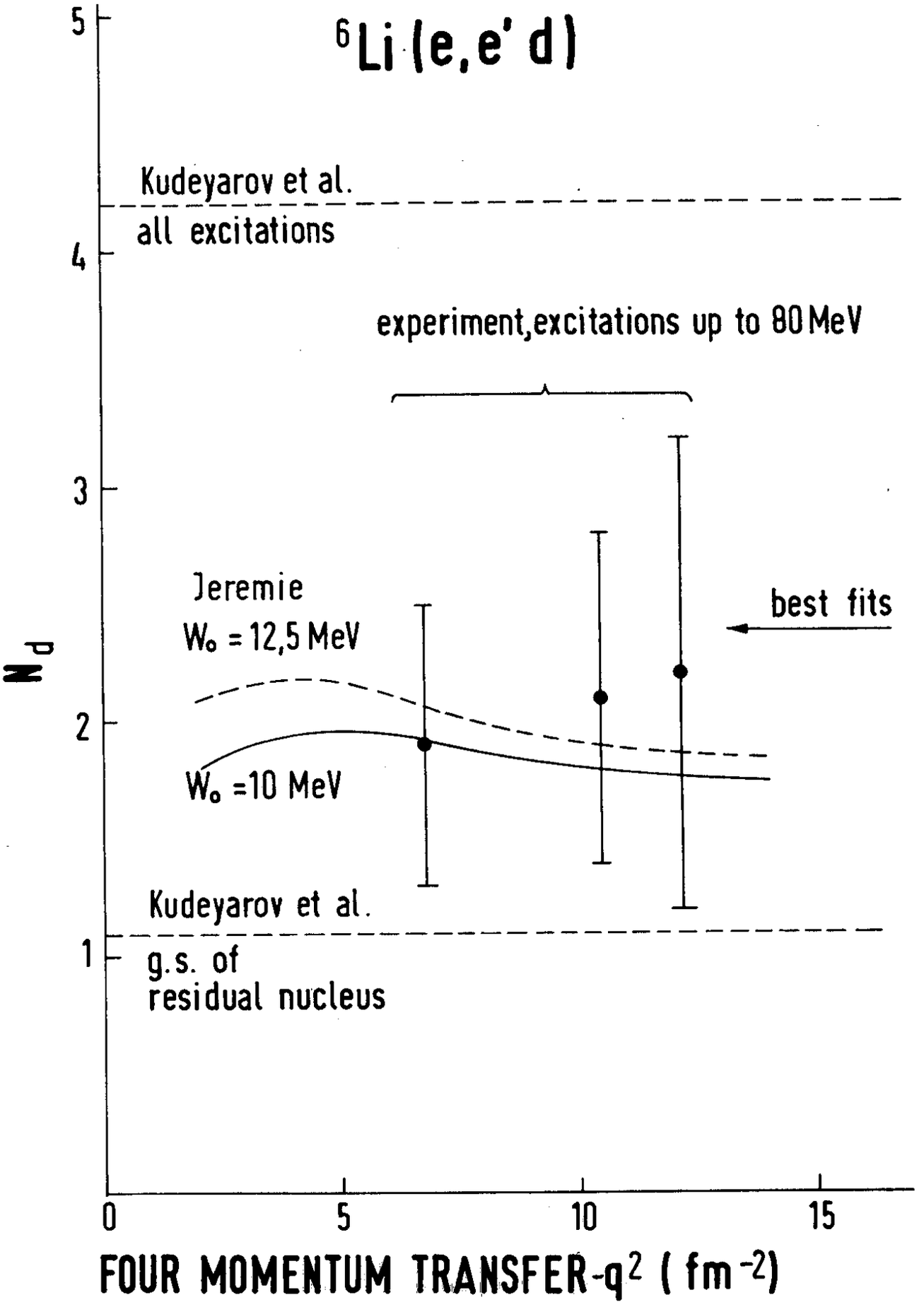
^{6}Li (e, e' d)
Kudeyarov et al.
all excitations
experiment, excitations up to 80 MeV
Jeremie
W_o = 12,5 MeV
W_o = 10 MeV
best fits
Kudeyarov et al.
g.s. of
residual nucleus
N_d
5
4
3
2
1
0
5
10
15
FOUR MOMENTUM TRANSFER $-q^2$ (fm^{-2})

FIG.5

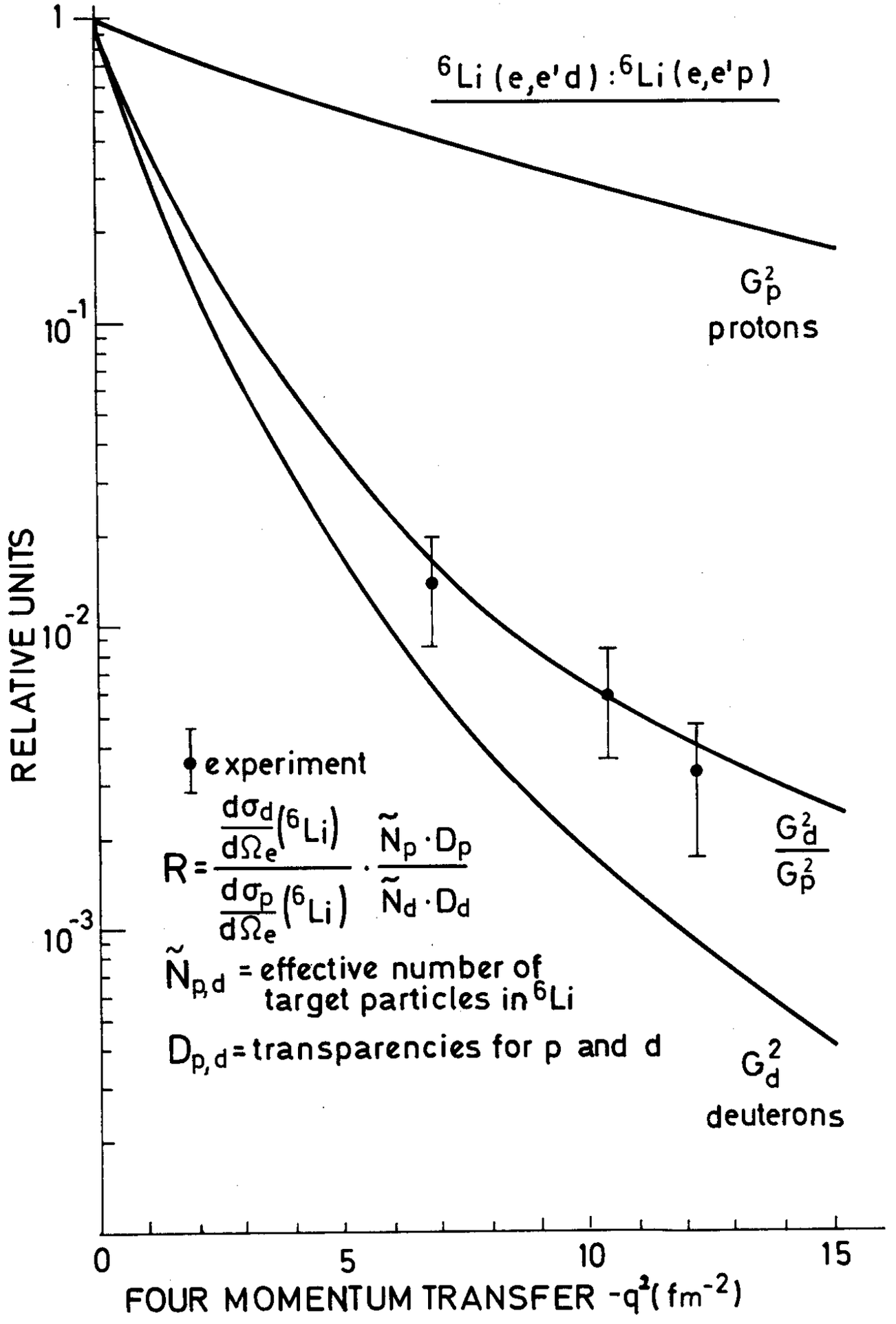
^{6}Li (e,e'd) : ^{6}Li (e,e'p)
G_p^2
protons
$\frac{G_d^2}{G_p^2}$
G_d^2
deuterons
experiment
$R = \frac{\frac{d\sigma_d}{d\Omega_e}(^6Li)}{\frac{d\sigma_p}{d\Omega_e}(^6Li)} \cdot \frac{\tilde{N}_p \cdot D_p}{\tilde{N}_d \cdot D_d}$
$\tilde{N}_{p,d}$ = effective number of target particles in ^{6}Li
$D_{p,d}$ = transparencies for p and d
RELATIVE UNITS
1
10^{-1}
10^{-2}
10^{-3}
0
5
10
15
FOUR MOMENTUM TRANSFER $-q^2$ (fm^{-2})

FIG.6